Open Access Full Text Article

ORIGINAL RESEARCH

# Dl-3-N-Butylphthalide Presents Anti-Cancer Activity in Lung Cancer by Targeting PD-1/PD-L1 Signaling

Qian Jiang[1–3]
Nan Zhang[2]
Xin Li[2]
Wei Hou[4]
Xiao-Qing Zhao[5]
Lei Liu[1,2]

[1]Department of Head and Neck Oncology, Department of Radiation Oncology, Cancer Center, West China Hospital of Sichuan University, Chengdu, 610041, Sichuan, People's Republic of China; [2]State Key Laboratory of Biotherapy, West China Hospital of Sichuan University, Chengdu, 610041, Sichuan, People's Republic of China; [3]Department of Oncology, Affiliated Hospital of North Sichuan Medical College, Nan Chong, 637000, Sichuan, People's Republic of China; [4]Department of Pathology, Affiliated Hospital of North Sichuan Medical College, Nan Chong, 637000, Sichuan, People's Republic of China; [5]Department of Oncology, The Second Affiliated Hospital of North Sichuan Medical College, Nan Chong, 637000, Sichuan, People's Republic of China

**Introduction:** Lung cancer serves as one of the most malignant cancer types. Immunotherapy targeting PD-1/PD-L1 axis is a promising strategy for cancer treatment. Dl-3-N-butylphthalide (NBP), a small molecule compound extracted from the seeds of Apium graveolens, possesses a large range of biological effects and demonstrates anti-cancer activities. However, the role of NBP in the modulation of lung cancer remains obscure.

**Methods:** In this study, we aimed to explore the effect of NBP on PD-L1 signaling and the progression of lung cancer.

**Results:** Significantly, the treatment of NBP repressed the proliferation of lung cancer cells in vitro. Tumorigenicity analysis in nude mice showed that the tumor volume and tumor weight were attenuated by the treatment of NBP in the mice. Meanwhile, the levels of Ki-67 and PD-L1 were reduced by the treatment of NBP in the tumor tissues of the mice. NBP suppressed IFN-γ-induced PD-L1 enhancement in lung cancer cells. The treatment of NBP inhibited PD-L1 expression in lung cancer cells co-cultured with unstimulated PBMCs or activated T cell. NBP inhibited PD-1 expression in activated T cells co-cultured with lung cancer cells. Conditioned medium from activated T cells increased PD-L1 expression, and NBP reversed this effect. Co-culture with A549 and H1975 cells reduced T cell proliferation and activity, while the treatment of NBP reversed the reduction. Consistently, the treatment of NBP caused notably decreased apoptosis of co-cultured T cells. Mechanically, KAT7 was able to bind to PD-L1 promoter and epigenetically induce PD-L1 expression by promoting the enrichment of histone H3 lysine 14 acetylation (H3K14ac) and RNA polymerase II on PD-L1 promoter.

**Discussion:** Thus, we concluded that NBP repressed PD-L1 expression by targeting KAT7 and attenuated PD-1/PD-L1 axis to relieve lung cancer progression. NBP may be applied as the potential therapeutic strategy in immunotherapy of lung cancer.

**Keywords:** lung cancer, Dl-3-N-butylphthalide, KAT7, PD-1/PD-L1 axis, immunotherapy

## Introduction

Lung cancer ranks one of the most malignant cancer types globally, with a 5-year survival rates less than 20%.[1] Despite of the great progresses for diagnostic techniques and therapeutic approaches in recent years, more than 70% of lung cancer patients are diagnosed with advanced metastatic disease, which are less responsive to curative therapy.[2]

Over the past decades, immune therapies have exhibited great potential in cancer therapy, among which the immune checkpoint inhibitors (ICIs) targeting the cytotoxic T lymphocyte associated antigen-4 (CTLA-4) and programmed death 1 (PD-1)/programmed death-ligand 1 (PD-L1) are widely studied in treatment for solid tumors.[3–5]

Correspondence: Lei Liu
Email liuleihx@gmail.com

**8513**

PD-L1 is a surface protein expressed by cancer cells and various immune cells, functionally recognize and interact with its cognate receptor that expressed by activated T cells, subsequently impeded the normal functions of T cells, and escaped from immune surveillance.[6,7] Numerous evidences have proved that targeting PD-1/PD-L1 signaling could partially recover the anti-tumor functions of activated T cells.[8,9] Studies demonstrated that PD-1/PD-L1 blockade treatment significantly improved the clinical response and prolonged survival rate without causing severe side effects, comparing with the traditional chemo- and radiotherapy.[10] Moreover, two PD-1 inhibitors, the pembrolizumab and nivolumab, were approved by the Food and Drug Administration (FDA) of USA for treatment of patients with metastatic non-small cell lung cancer (NSCLC) and progressed after platinum-based therapy.[11,12] Nevertheless, there exists great challenges for the further application of ICIs in clinical practice such as limited patient group, primary or acquired resistance, and immune-related adverse reactions.[13–15] Therefore, discovering effective and safe approaches to block PD-1/PD-L1 axis is of great clinical value for lung cancer therapy.

Dl-3-N-butylphthalide (NBP) is a small molecule extract initially obtained from the seeds of celery, and approved as clinical drug for ischemic stroke by the State Food and Drug Administration of China in 2002 owing to its high safety and effectiveness.[16] Studies have revealed that NBP participated in the regulation of inflammation, apoptosis, oxidative stress response, mitochondrial function and neuroprotection.[17–19] For example, NBP suppressed the cerebral ischemia-induced inflammatory response via blocking the NF-κB signaling transduction.[20,21] As for application in tumor therapies, NBP was reported to perform cytotoxic activity and suppress invasion of hepatocellular carcinoma cells.[22] Yet the function of NBP in lung cancer is unclear.

In this work, we aimed to determine the function of NBP in lung cancer, and disclosed decreased expression of PD-1 and PD-L1 in activated T cells and lung cancer cells, respectively. Mechanism study revealed an epigenetic regulation of PD-L1 under NBP treatment. These findings suggested NBP as a promising therapeutic agent for lung cancer immune therapy.

# Materials and Methods
## Ethical Statement
The protocol was approved by the West China Hospital of Sichuan University. All subjects gave written informed consent in accordance with the Declaration of Helsinki. Written informed consent have been provided by the donor.

## Cell Lines and Materials
Human lung cancer cell line A549, H1975 and murine Lewis lung cancer (LLC) cells were purchased from American Type Culture Collection (ATCC, USA) and cultured in 10% fetal bovine serum (FBS, Gibco)-containing DMEM at a 37 °C humidified atmosphere filled with 5% $CO_2$. Co-culture was conducted by using 0.4 μm-pore Transwell system (Costar, USA). The cancer cells were placed in the bottom chamber before the seeding of T cells into the top chamber. Conditioned medium (CM) was collected from the culture medium through centrifuge with 12,000 rpm for 15 minutes at 4 °C. The collected CM was then applied to cell culture at a ratio of 1:1 with fresh medium. NBP with a purity of 99% was obtained from Shijiazhuang Pharma Group, dissolved in DMSO at a storage concentration of 50 mg/mL, and diluted in water before cellular (5 μM) or animal experiments (80 mg/kg).

## Cell Transfection
Small hairpin RNA targeting KAT7 (shKAT7), PD-L1 (shPD-L1), and the negative control (shNC) were purchased from RiboBio (China). A549 and H1975 cells were transfected with shRNAs via Lipofectamine 2000 in line with manufacturer's protocol.

## T Cell Priming
Blood samples were collected from healthy donors, and peripheral blood mononuclear cells (PBMCs) were isolated in accordance with the instruction of Ficoll method. For isolation of T cells from the PBMCs, we used a Pan-T cell isolation kit (Miltenyi Biotec, Germany) under the manufacturer's description. The T Cell Activation/Expansion Kit (Miltenyi Biotec) was adopted to activate the isolated T cells in line with the manufacturer's protocol. In short, biotin-labelled CD2, CD3 and CD28 antibodies were conjugated to MACS Beads, followed by administration to the isolated cells.

## Cell Viability, Proliferation and Apoptosis
Cell counting kit-8 (Thermo, USA), colony formation, and 5-ethynyl-2′-deoxyuridine (EdU) experiment were established to determine the viability and proliferative ability of cells. For CCK-8 assay, cells were seeded in 96-well plates, followed by culture for 24, 48, or 72 hours. CCK-8 reagent (15 μL) was then added into each well to incubate for 1 hour, the absorbance at optical density

(OD) 450 nm were evaluated by a microplate reader (BD Biosciences, USA).

To establish colony formation assay, A549 and H1975 cells (500 cells per well) were planted in 12-well plates and placed in 37°C incubator for two weeks. Medium were changed every three days. The colonies were fixed with methanol and dyed by 0.2% crystal violet for 15 minutes. Images of whole well were taken by a camera.

For EdU evaluation of DNA replication, cells were fixed in 4% PFA and permeabilized with Triton X-100, then incubated with EdU reagent (50 μM, RiboBio) for 3 hours. Nuclei were labelled with Hoechst 33342. Five random areas were captured by a confocal microscope.

Cell apoptosis was evaluated by flow cytometry by using FITC-Annexin V/PI detection kit (Beyotime, China) following the manufacturer's protocol. In short, cells were collected and stained with FITC-Annexin V (5 μL) and PI (5 μL) in dark for 15 minutes, followed by detection on a Calibur C6 system.

## Xenograft Mice Model

All experimental procedures were authorized by Animal Care and Use Committee of West China Hospital of Sichuan University, and carried out in accordance with the National Institutes of Health guide for the care and use of Laboratory animals (NIH Publications No. 8023, revised 1978). Male C57BL/6J mice aged 4–6 weeks were obtained from the Vital River Laboratory (Beijing), and housed in specific pathogen-free environment with free access to food and water. A total number of $5 \times 10^5$ LLC cells were injected into the right-side flank of each mouse. When tumor size reached the size of around 100 mm³, mice were randomly separated into experimental groups and received corresponding treatment. Mice in PD-L1 treatment group received intraperitoneal injection (IP) of anti-PD-L1 (Abcam, 5 mg/kg) at day 1, 3 and 7 after grouping. Butylphthalide treatment (80 mg/kg) was performed every day through intragastric administration. The mice in control group received injection of murine total-IgG and saline as control. Tumor size and mice body weight were recorded every three days.

## Immunohistochemical (IHC) Analysis

For IHC analysis of proliferation marker Ki-67, tumors were collected, paraffin-embedded and made into 4-μm thick sections. After antigen retrieval by heating, blockade of endogenous peroxidase activity with 3% solution of hydrogen peroxide, the tissue sections were blocked with 5% bovine serum albumin (BSA) and incubated with anti-

Ki67 antibody for one night at 4 °C. Next day, the tissues were visualized by 3,3-diaminobenzidine (DAB).

## Quantitative Real-Time PCR

To analyze the change of PD-L1 and KAT7 expression, total RNAs were obtained by homogenizing cells using Trizol reagent, transcribed to cDNAs by Reverse Transcription System Reagent Kit (Promega, USA). The quantification of gene expression was established by using SYBR Green Master kit following manufacturer's protocol and calculated following the $2^{-\Delta\Delta Ct}$ method. β-Actin was adopted as the internal reference gene. The primers for target genes were listed as follows:

KAT7, forward primer, 5′-ATTCTGGACTGAGCAAAGAACAG-3′, and reverse primer, 5′-GTCATACTCGCTTGTCAGGTTTT-3′;

PD-L1, forward primer, 5′- GCCGAAGTCATCTGGACAAG-3-3′, and reverse primer,5′-TCTCAGTGTGCTGGTCACAT-3′.

## Flow Cytometry Analysis

To detect the expression of cell surface biomarkers including PD-L1, CD4 and CD8, cells were suspended in PBS (100 μL) that contained 3% FBS, then stained with FITC anti-PD-L1, APC anti-CD8, PE anti-CD4, FITC anti-PD-1, or isotype control on ice avoiding light for 30 minutes. After that, cells were washed and detected on the FACS Calibur C6. The level of PD-L1 was shown as the mean fluorescence intensity (MFI).

## Chromatin Immunoprecipitation (ChIP)

Interaction between proteins and the promoter region of PD-L1 was detected by ChIP assay using a ChIP assay kit under the instruction of manufacturer. In short, A549 and H1975 cells were crosslinked in 1% formaldehyde and lysed to obtain genome DNA. After sonication, the genome was fractured to fragments around 500 bp by sonication, then hatched with the specific antibodies against KAT7, H3K14Ac, H3K27Ac, RNA polymerase II, or IgG as control in rotation at 4°C overnight. The samples were then incubated with Dynabeads for one hour at 4°C. The samples were then eluted by incubation with proteinase K, and enriched DNAs were quantified by PCR.

## Statistics

The data were presented as mean ± standard deviation (SD) of three independent replicates. Statistical differences were analyzed by two-tailed Student's *t*-test or one-way
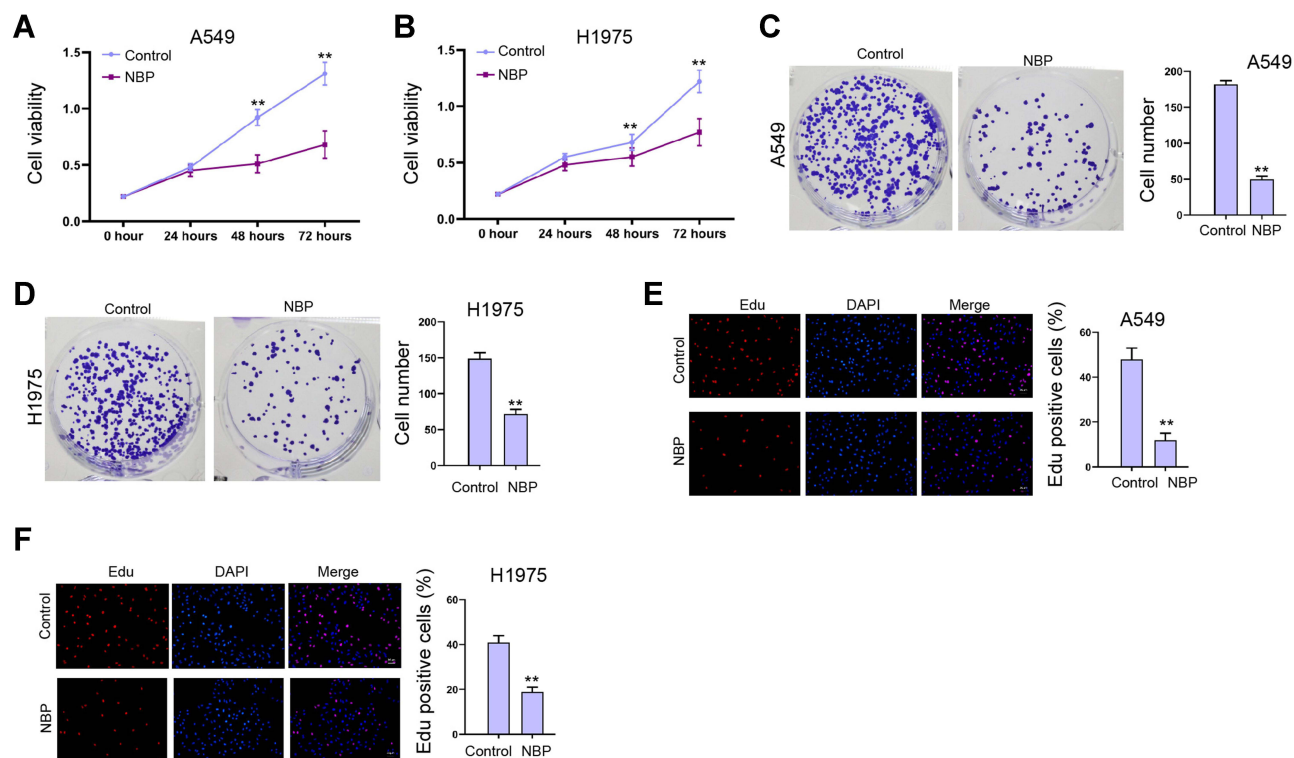
**Figure 1** NBP represses proliferation of lung cancer cells. (**A–F**) The A549 and H1975 cells were treated with NBP. (**A** and **B**) The cell viability was measured by CCK-8 assays. (**C** and **D**) The cell proliferation was detected by colony formation assays. (**E** and **F**) The cell proliferation was analyzed by Edu assay. mean ± SD. **$P < 0.01$.

ANOVA using GraphPad Prism 7 software, and $p$ value < 0.05 was regarded as statistically significant.

## Results
### NBP Represses Proliferation of Lung Cancer Cells

Given that the function of NBP in the modulation of lung cancer cell proliferation is still unclear, we evaluated the effect of NBP on the cell proliferation of A549 and H1975 cells in vitro. Significantly, CCK-8 assays showed that the viabilities of A549 and H1975 cells were inhibited by NBP (Figure 1A and B). Meanwhile, A549 and H1975 cell colony formation numbers were decreased by NBP (Figure 1C and D). The Edu-positive cells were reduced by NBP in A549 and H1975 cells (Figure 1E and F), indicating that NBP represses proliferation of lung cancer cells.

### NBP Inhibits Lung Cancer Cell Growth in vivo

Then, we verified the function of NBP in the modulation of lung cancer cell growth in vivo. Tumorigenicity analysis in nude mice showed that the tumor volume and tumor weight were attenuated by the treatment of NBP in the mice

(Figure 2A and B). Meanwhile, the levels of Ki-67 and PD-L1 were reduced by the treatment of NBP (Figure 2C and D).

### NBP Reduces IFN-γ-Induced PD-L1 Enhancement in Lung Cancer Cells

Given that interferon-γ (IFN-γ) was a strong inducer of PD-L1, we further evaluated the effect of NBP on IFN-γ-mediated PD-L1 expression. As expected, the treatment of IFN-γ remarkably increased the expression of PD-L1 in A549 and H1975 cells (Figure 3A and B). Meanwhile, the A549 and H1975 cells were treated with IFN-γ or co-treated with IFN-γ and NBP. We observed that NBP significantly impaired the IFN-γ-induced PD-L1 expression in A549 and H1975 cells (Figure 3C and D). Besides, we validated that the treatment of NBP could reduce PD-L1 expression in A549 and H1975 cells (Figure 3E).

### NBP Stimulates T Cells Activity and Proliferation to Suppresses Lung Cancer Cell Survival

Next, we tried to explore whether NBP affected T cell function in a Transwell T cells/lung cancer cells co-cultured system. The unstimulated or activated T cells were placed in upper
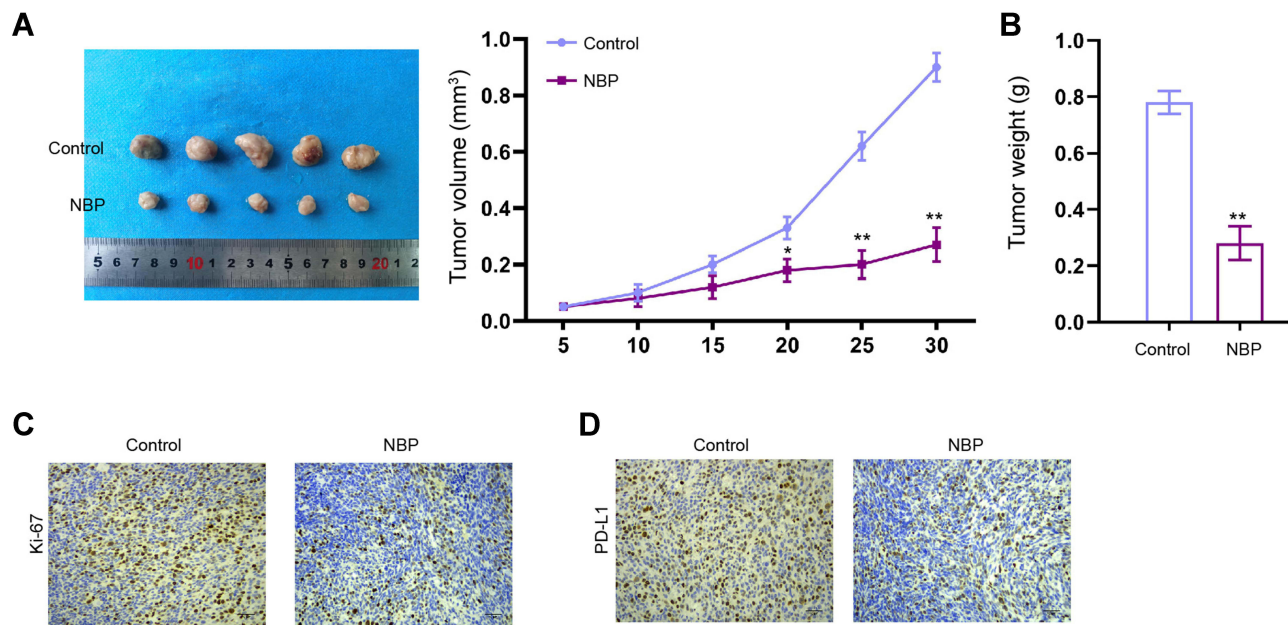
**Figure 2** NBP inhibits lung cancer cell growth in vivo. (**A–D**) The nude mice were injected with A549 cells and treated with NBP. The cell growth of was analyzed by tumorigenicity analysis in the nude mice. (**A**) The tumor volume was calculated. (**B**) The tumor weight was calculated. (**C**) The levels of Ki-67 were detected by IHC. (**D**) The expression of PD-L1 was tested by IHC. N=5, mean ± SD. *$P$ < 0.05, **$P$ < 0.01.
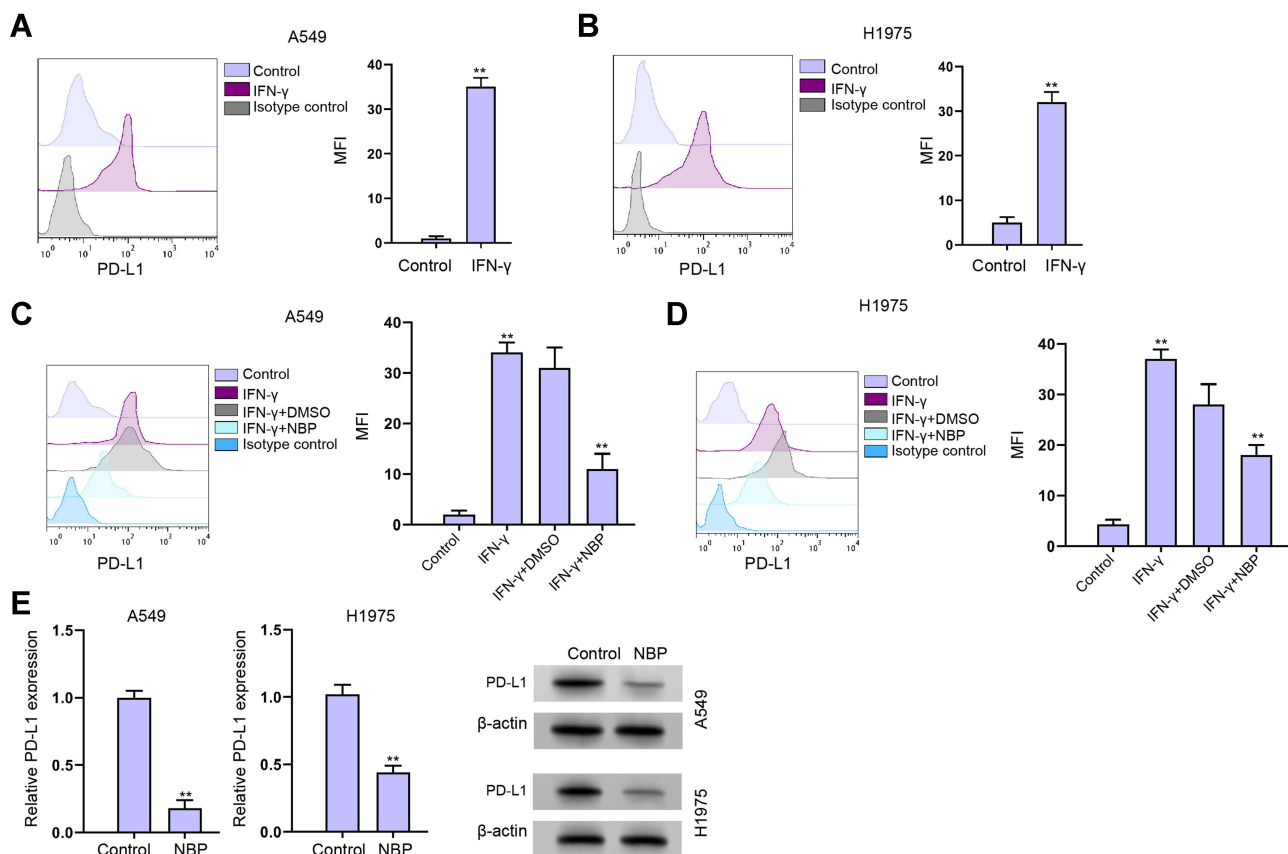


**Figure 3** NBP reduces IFN-γ-induced PD-L1 enhancement in lung cancer cells. (**A** and **B**) The A549 and H1975 cells were treated with IFN-γ (200 ng/mL). The expression of PD-L1 was analyzed by fluorescence-activated cell sorting (FACS) in the cells. (**C** and **D**) The A549 and H1975 cells were treated with IFN-γ (200 ng/mL), or co-treated with IFN-γ (200 ng/mL) and NBP. The expression of PD-L1 was analyzed by FACS in the cells. (**E**) The expression of PD-L1 was determined by qPCR in A549 and H1975 cells treated with NBP. mean ± SD. **$P$ < 0.01.
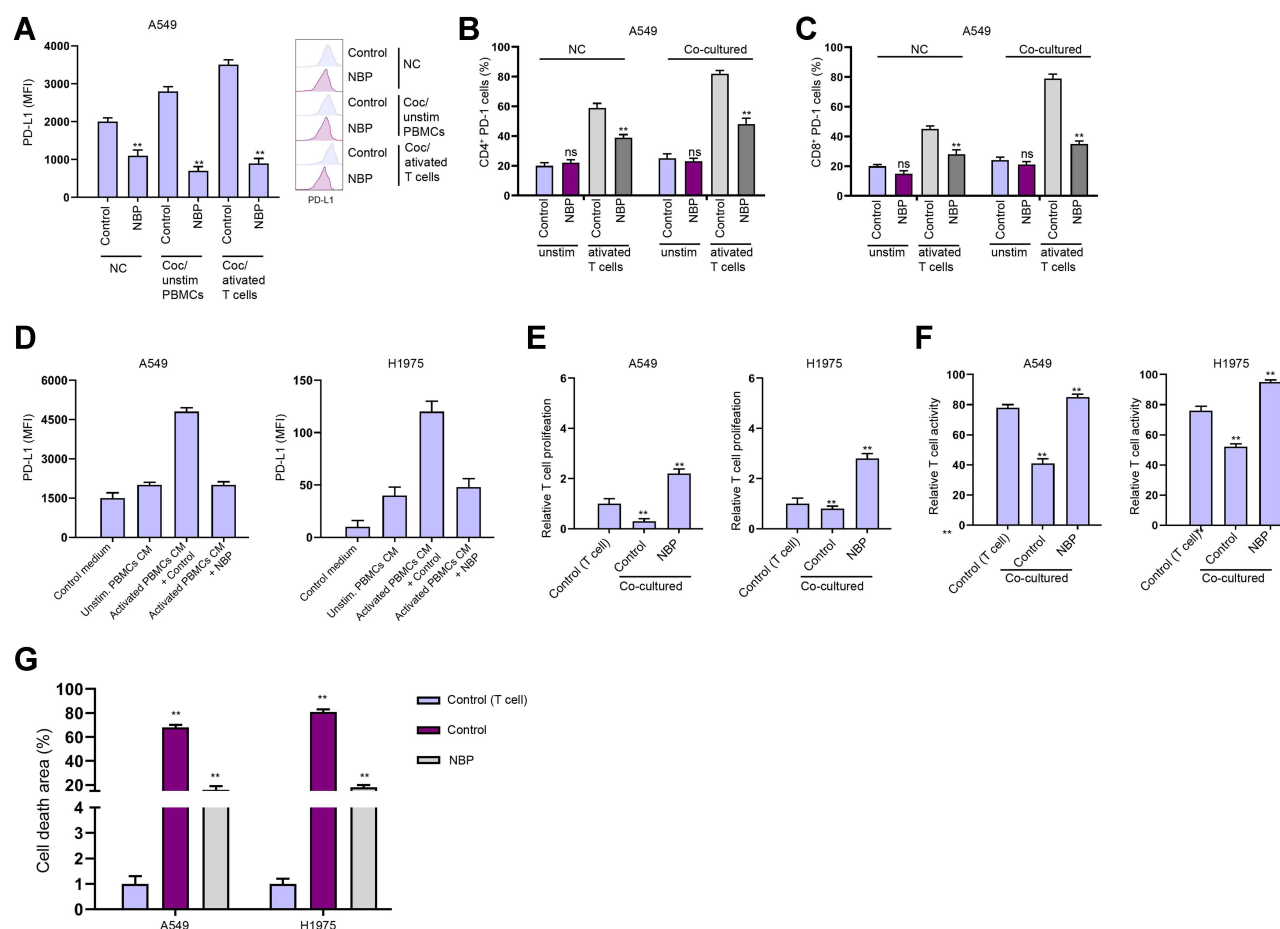
**Figure 4** NBP stimulates T cells activity and proliferation to suppresses lung cancer cell survival. (**A**–**E**) The co-culture system was established by placing the unstimulated or activated T cells in upper chambers of the Transwell, and the A549 and H1975 cells in the lower chambers at a ratio of 1:10. (**A**) The expression of PD-L1 was analyzed by FACS in the cells. (**B** and **C**) The proportions of CD4$^+$ PD-1$^+$ and CD8$^+$ PD-1$^+$ T cell were determined by flow cytometry. (**D**) Expression of PD-L1 in A549 and H1975 cells cultured in conditioned medium from unstimulated or activated PBMCs. (**E**) T cell proliferation under co-cultured with A549 and H1975 cells was determined by CCK-8 assay. (**F**) T cell activity under co-cultured with A549 and H1975 cells was determined by flow cytometry detection of CD8$^+$ T cells. (**G**) Apoptosis of T cells was determined by flow cytometry. mean ± SD. \*\*$P < 0.01$.
**Abbreviation**: Ns, not significant.

chambers of the Transwell, the A549 and H1975 cells were set in the lower chambers. We validated that the treatment of NBP inhibited PD-L1 expression in A549 co-cultured with unstimulated PBMCs or activated T cells (Figure 4A). NBP suppressed PD-1 expression in activated T cells under co-culture with A549 and H1975 cells (Figure 4B and C). To confirm the possibility that T cells regulate lung cancer cell function through secreting factors, we treated A549 and H1975 cells with the culture medium collected from PBMCs. We found that culture under the conditioned medium from activated T cells increased PD-L1 expression, and NBP reversed this effect (Figure 4D). Results from CCK-8 and flow cytometry demonstrated that co-culture with A549 and H1975 cells significantly reduced T cell proliferation and activity, while the treatment of NBP reversed the reduction (Figure 4E and F). Consistently, the treatment of NBP caused notably decreased

apoptosis of co-cultured T cells, comparing with that in the NC group (Figure 4G).

## NBP Suppresses PD-L1 Expression in Lung Cancer Cells Through Targeting KAT7

We then explored the underlying mechanism of NBP repressing PD-L1 expression in lung cancer cells. We identified that NBP was able to reduce KAT7 expression in A549 and H1975 cells (Figure 5A). Meanwhile, the effectiveness of KAT7 depletion by shRNAs was validated in A549 and H1975 cells, in which shRNA-1 showed a higher efficiency and was used in the subsequent experiments (Figure 5B). We found that the expression of PD-L1 was reduced by KAT7 knockdown in A549 and H1975 cells (Figure 5C). KAT7 was able to enrich in the promoter of PD-L1, while the treatment of NBP decreased this enrichment (Figure 5D). The levels of histone H3 lysine 14
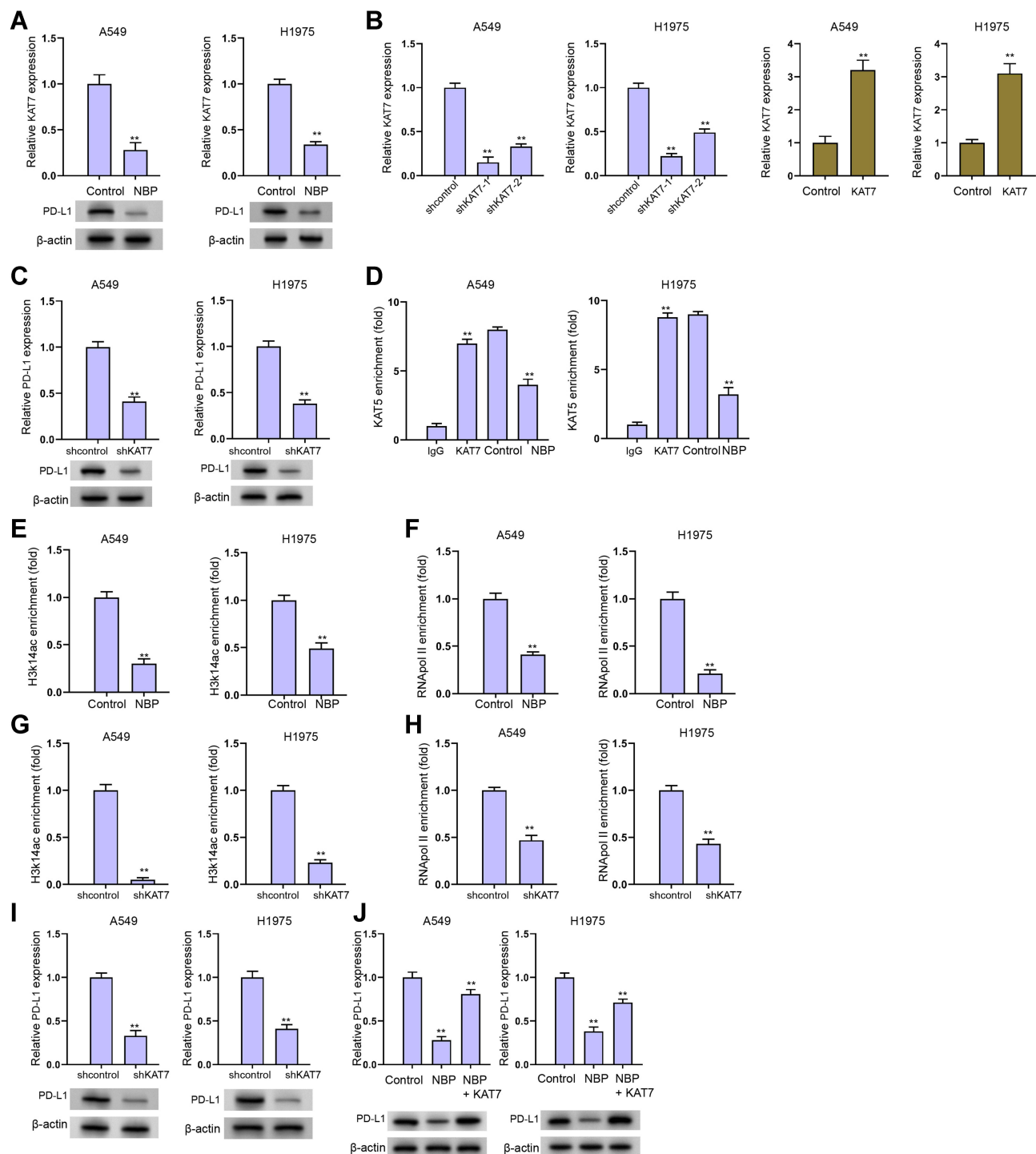
**Figure 5** NBP suppresses PD-L1 expression in lung cancer cells through targeting KAT7. (**A**) The expression of KAT7 was analyzed by qPCR in A549 and H1975 cells treated with NBP. (**B**) The expression of KAT7 was determined by qPCR in A549 and H1975 cells treated with KAT7 shRNAs. (**C**) The expression of PD-L1 was determined by qPCR in A549 and H1975 cells treated with KAT7 shRNA. (**D–F**) The A549 and H1975 were cells treated with NBP. The enrichment of KAT7 (**D**), H3K14ac (**E**), and RNA pol II (**F**) on PD-L1 promoter was analyzed by ChIP assays. (**G–I**) The A549 and H1975 were cells treated with NBP. The enrichment of KAT7 (**G**) and H3K14ac (**H**), on PD-L1 promoter was analyzed by ChIP assays. (**I**) The expression of PD-L1 was determined by qPCR. (**J**) The expression of PD-L1 was detected by qPCR in A549 and H1975 cells treated with NBP or co-treated with NBP and KAT7 overexpressing plasmid. mean ± SD. **$P$ < 0.01.
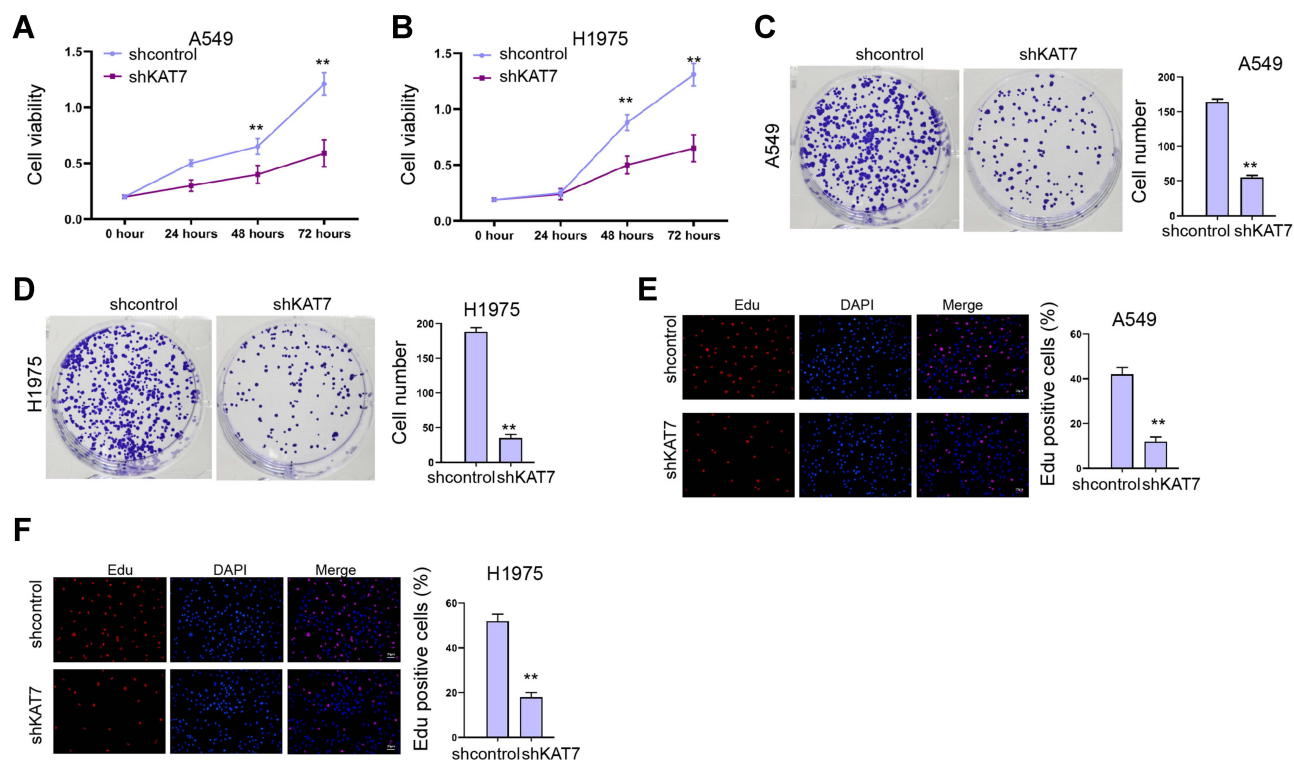
**Figure 6** The depletion of KAT7 reduces proliferation of lung cancer cells. (**A**–**F**) The A549 and H1975 cells were treated with KAT7 shRNA. (**A** and **B**) The cell viability was measured by CCK-8 assays. (**C** and **D**) The cell proliferation was detected by colony formation assays. (**E** and **F**) The cell proliferation was analyzed by Edu assay. mean ± SD. **$*P < 0.01$.

acetylation (H3K14ac) and RNA polymerase II on PD-L1 promoter were decreased by NBP in A549 and H1975 cells (Figure 5E and F). Meanwhile, the levels of H3K14ac, RNA polymerase II on PD-L1 promoter and the expression of PD-L1 were downregulated by the depletion of KAT7 in A549 and H1975 cells (Figure 5G–I). The NBP-repressed expression of PD-L1 could be restored by the overexpression of KAT7 in A549 and H1975 cells (Figure 5J), indicating that NBP suppresses PD-L1 expression in lung cancer cells through targeting KAT7.

## The Depletion of KAT7 Reduces Proliferation of Lung Cancer Cells

Then, we validated the effect of KAT7 on the cell proliferation of A549 and H1975 cells in vitro. The viabilities of A549 and H1975 cells were inhibited by the depletion of KAT7 (Figure 6A and B). Meanwhile, A549 and H1975 cell colony formation numbers were decreased by KAT7 knockdown (Figure 6C and D). The Edu-positive cells were reduced by KAT7 silencing in A549 and H1975 cells (Figure 6E and F), indicating that the depletion of KAT7 reduces proliferation of lung cancer cells.

## The Depletion of KAT7 Stimulates T Cells Activity and Proliferation to Suppresses Lung Cancer Cell Survival

Next, we investigated the effect of KAT7 on T cell function in a Transwell T cells/lung cancer cells co-cultured system. We confirmed that the depletion of KAT7 repressed PD-L1 expression in A549 co-cultured with unstimulated PBMCs or activated T cells (Figure 7A). KAT7 knockdown inhibited PD-1 expression in activated T cells under co-culture with A549 and H1975 cells (Figure 7B and C). Conditioned medium from activated T cells increased PD-L1 expression, and KAT7 knockdown reversed this effect (Figure 7D). Co-culture with A549 and H1975 cells significantly reduced T cell proliferation and activity, while the silencing of KAT7 reversed the reduction (Figure 7E and F). Consistently, the depletion of KAT7 attenuated apoptosis of co-cultured T cells (Figure 7G).

## NBP Reverses KAT7 Overexpression-Inhibited T Cells Activity and Proliferation

Then, we determined the correlation of NBP and KAT7 in the modulation of T cells. We identified that co-culture with
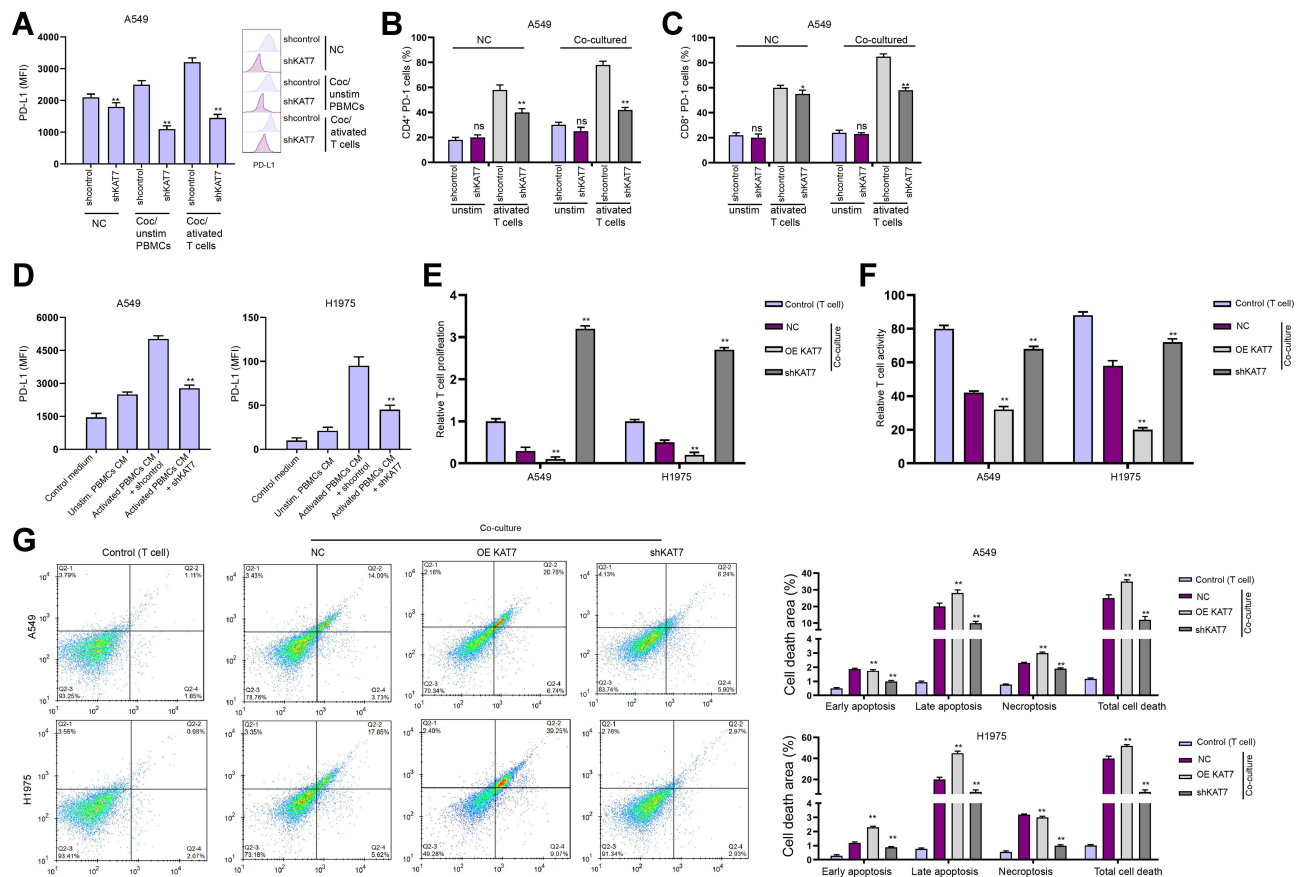
**Figure 7** The depletion of KAT7 stimulates T cells activity and proliferation to suppresses lung cancer cell survival. (**A–E**) The co-culture system was established by placing the unstimulated or activated T cells in upper chambers of the Transwell, and the A549 and H1975 cells treated with KAT7 shRNA in the lower chambers at a ratio of 1:10. (**A**) The expression of PD-L1 was analyzed by FACS in the cells. (**B** and **C**) The proportions of CD4$^+$ PD-1$^+$ and CD8$^+$ PD-1$^+$ T cell were determined by flow cytometry. (**D**) Expression of PD-L1 in A549 and H1975 cells cultured in conditioned medium from unstimulated or activated PBMCs. (**E**) T cell proliferation under co-cultured with A549 and H1975 cells was determined by CCK-8 assay. (**F**) T cell activity under co-cultured with A549 and H1975 cells was determined by flow cytometry detection of CD8$^+$ T cells. (**G**) Apoptosis of T cells was determined by flow cytometry. mean ± SD. *$P < 0.05$, **$P < 0.01$.
**Abbreviation**: ns, not significant.

A549 and H1975 cells significantly reduced T cell proliferation and activity, while the overexpression of KAT7 reduced the T cell proliferation and activity co-cultured with A549 and H1975 cells, while the treatment of NBP reversed this reduction (Figure 8A and B). The overexpression of KAT7-induced apoptosis of co-cultured T cells and the treatment of NBP blocked the effect (Figure 8C).

## NBP Improves Anti-PD-L1 Immunotherapy Against Lung Cancer Cell Growth in vivo

Subsequently, we analyzed the combined effect of NBP with anti-PD-L1 immunotherapy on lung cancer cell growth in vivo. Our data revealed that anti-PD-L1 monoclonal antibody was able to repress the tumor growth of murine Lewis lung cancer (LLC) cells in C57BL/6 mice, while the co-treatment of anti-PD-L1 monoclonal antibody and NBP significantly improved the inhibitory effect on the tumor growth in the system, as demonstrated by the tumor size, tumor volume, tumor weight, Ki-67 and PD-L1 levels (Figure 9A–D).

## Discussion

Lung cancer is one of the most malignant cancer types with high mortality and poor prognosis globally. Immunotherapy targeting PD-1/PD-L1 axis is a promising strategy for cancer treatment. NBP possesses a large range of biological effects and demonstrates anti-cancer activities. However, the function of NBP in the modulation of lung cancer remains obscure. In this study, we aimed to explore the effect of NBP on PD-L1 signaling and the progression of lung cancer.
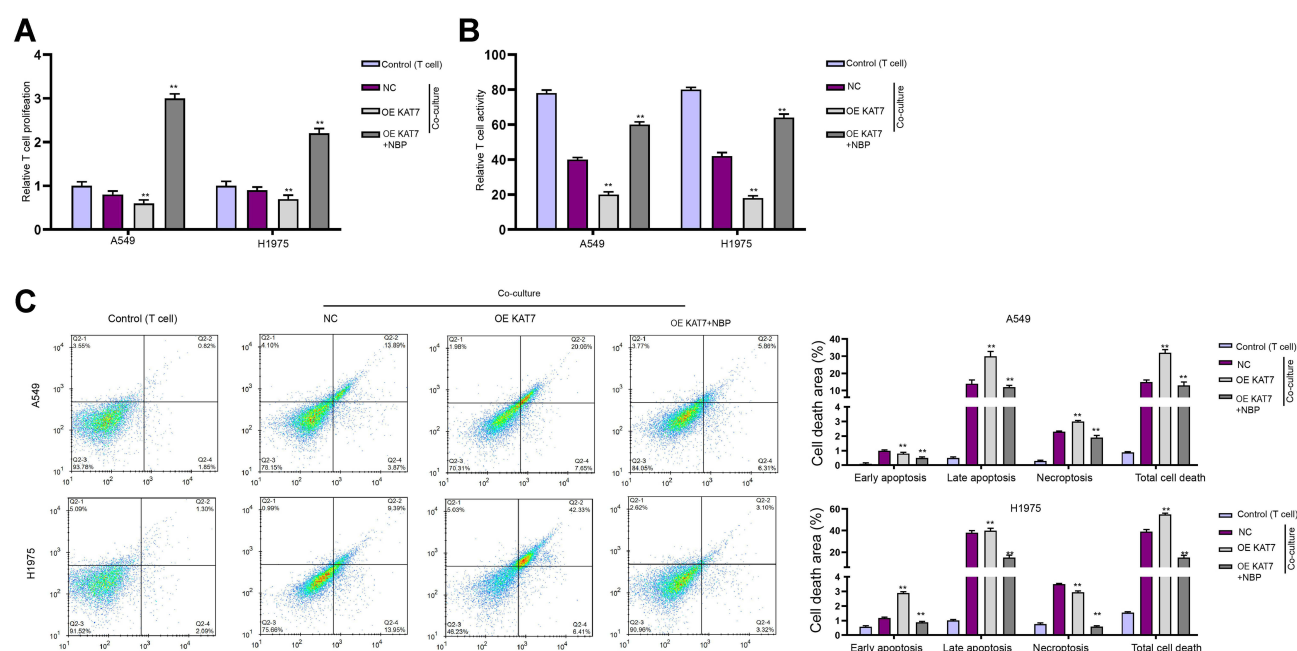
**Figure 8** NBP reverses KAT7 overexpression-inhibited T cells activity and proliferation. (**A–C**) The co-culture system was established by placing the unstimulated or activated T cells in upper chambers of the Transwell, and the A549 and H1975 cells treated with KAT7 overexpressing plasmid or co-treated with NBP in the lower chambers at a ratio of 1:10. (**A**) T cell proliferation under co-cultured with A549 and H1975 cells was determined by CCK-8 assay. (**B**) T cell activity under co-cultured with A549 and H1975 cells was determined by flow cytometry detection of CD8+ T cells. (**C**) Apoptosis of T cells were determined by flow cytometry. mean ± SD. **$P < 0.01$.
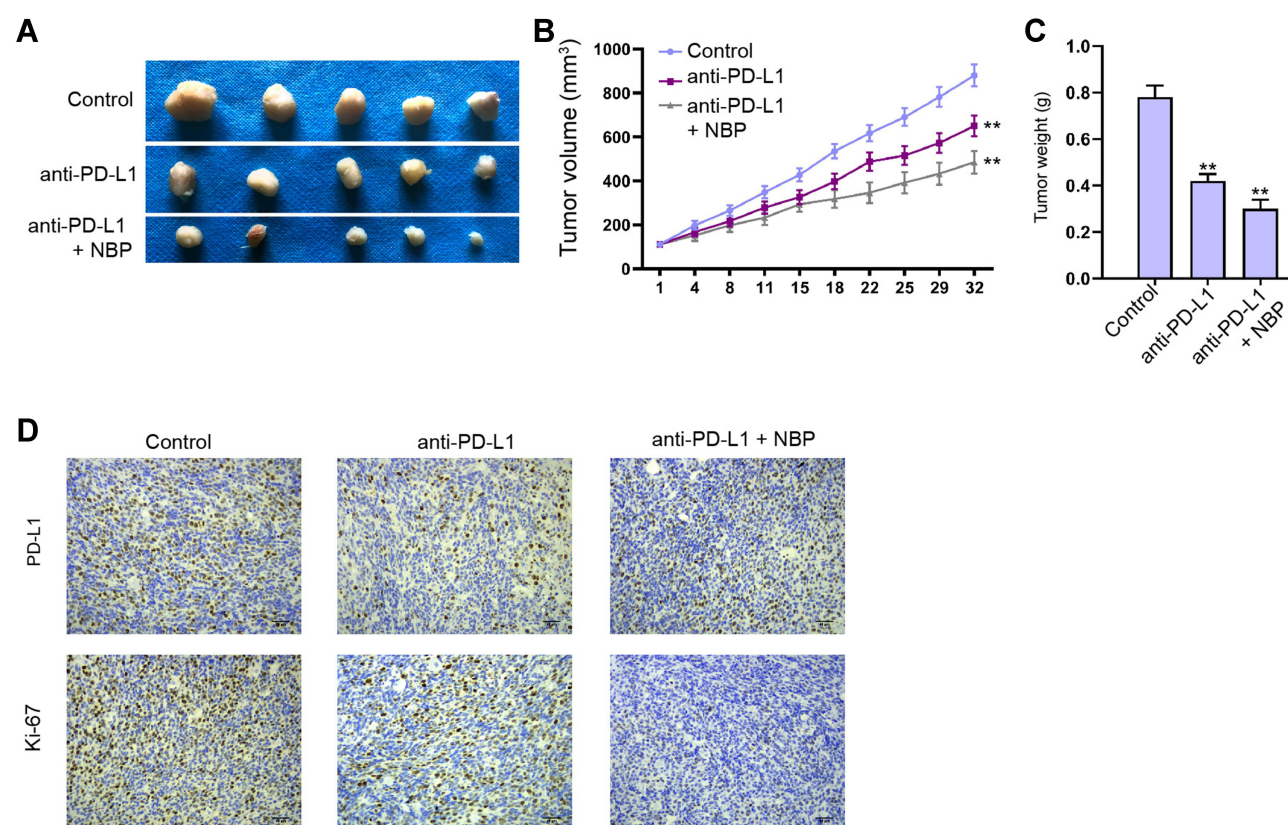


**Figure 9** NBP improves anti-PD-L1 immunotherapy against lung cancer cell growth in vivo. (**A–D**) C57BL/6 mice were subcutaneously injected with murine Lewis lung cancer (LLC) cells. The mice accepted injection of the anti PD-L1 monoclonal antibody, or co-treated with anti PD-L1 monoclonal antibody and NBP. (**A**) The tumor images were shown. (**B**) The tumor volume was calculated. (**C**) The tumor weight was calculated. (**D**) The levels of Ki-67 and PD-L1 were detected by IHC. N=5, mean ± SD. **$P < 0.01$.

The previous studies have identified the potential biomedical effect of NBP in multiple diseases. NBP enhances lipopolysaccharide-stimulated depressive-like function by targeting Nrf2 and NF-κB signaling.[23] NBP attenuates methamphetamine-related neurotoxicity in neuroblastoma cells.[24] NBP protects against doxorubicin-stimulated endoplasmic reticulum stress, oxidative stress, neuroinflammation, and behavioral changes.[25] Meanwhile, several natural compounds have presented the anti-cancer function by targeting PD-L1 in cancer progression. Resveratrol regulates dimerization and glycosylation of PD-L1 to induce anti-tumor T-cell immunity.[26] Bioactive gallic acid inhibits PD-L1 expression to represses lung cancer progression.[27] Panaxadiol suppresses PD-L1 expression and colon cancer cell proliferation by targeting STAT3 and hypoxia-inducible factor (HIF)-1α.[28] In this study, we found the treatment of NBP repressed the proliferation of lung cancer cells in vitro. Tumorigenicity analysis in nude mice showed that the tumor volume and tumor weight were attenuated by the treatment of NBP in the mice. Meanwhile, the levels of Ki-67 and PD-L1 were reduced by the treatment of NBP in the tumor tissues of the mice. NBP suppressed IFN-γ-induced PD-L1 enhancement in lung cancer cells. The treatment of NBP inhibited PD-L1 expression in lung cancer cells co-cultured with unstimulated PBMCs or activated T cells. NBP inhibited PD-1 expression in activated T cells co-cultured with lung cancer cells. Conditioned medium from activated T cells increased PD-L1 expression, and NBP reversed this effect. Co-culture with A549 and H1975 cells reduced T cell proliferation and activity, while the treatment of NBP reversed the reduction. Consistently, the treatment of NBP caused notably decreased apoptosis of co-cultured T cells. These data suggest that NBP could induce inhibitory effect on lung cancer progression by targeting PD-1/PD-L1. Our finding provides new evidence of the critical roles of NBP in cancer progression. The clinical significance of NBP should be explored in future investigations.

Moreover, the function of KAT7 in cancer development have been reported. It has been found that circMRPS35 inhibits progression of gastric cancer by regulating KAT7 to mediate histone modification.[29] KAT7 contributes to the maintenance of leukaemia stem cell properties.[30] KAT7 regulates histone H4 acetylation to potentiate membrane elasticity and echano-transduction signaling in ovarian cancer.[31] In the present investigation, we found that KAT7 was able to bind to PD-L1 promoter and epigenetically induce PD-L1 expression by promoting

the enrichment of histone H3 lysine 14 acetylation (H3K14ac) and RNA polymerase II on PD-L1 promoter, while NBP could block the recruitment of KAT7 PD-L1 promoter and repress PD-L1 expression by inhibiting KAT7. We validated that the depletion of KAT7 reduced proliferation of lung cancer cells and stimulated T cells activity and proliferation. NBP reversed KAT7 overexpression-inhibited T cells activity and proliferation. Moreover, NBP improved anti-PD-L1 immunotherapy against lung cancer cell growth in vivo. These data uncover a significant function of KAT7 in regulation of PD-1/PD-L1 axis in lung cancer progression, presenting the crucial effect of KAT7 on PD-1/PD-L1-related immune microenvironment of lung cancer and providing a potential strategy of immunotherapy for lung cancer at the experimental condition. Our finding proves new insight into the mechanism by which NBP represses lung cancer progression through targeting KAT7/PD-L1 axis. The clinical significance of KAT7 needs to be explored in future investigations.

Taken together, we concluded that NBP repressed PD-L1 expression by targeting KAT7 and attenuated PD-1/PD-L1 axis to relieve lung cancer progression. NBP may be applied as the potential therapeutic strategy in immunotherapy of lung cancer.

## Disclosure

The authors declare no competing financial interests.

## References

1. Siegel RL, Miller KD, Jemal A. Cancer statistics, 2020. *CA Cancer J Clin*. 2020;70(1):7–30. doi:10.3322/caac.21590
2. Ettinger DS, Wood DE, Akerley W, et al. NCCN guidelines insights: non–small cell lung cancer, version 4.2016. *J Natl Compr Canc Netw*. 2016;14(3):255–264. doi:10.6004/jnccn.2016.0031
3. Curran MA, Montalvo W, Yagita H, Allison JP. PD-1 and CTLA-4 combination blockade expands infiltrating T cells and reduces regulatory T and myeloid cells within B16 melanoma tumors. *Proc Natl Acad Sci U S A*. 2010;107(9):4275–4280. doi:10.1073/pnas.0915174107
4. Conway JR, Kofman E, Mo SS, Elmarakeby H, Van Allen E. Genomics of response to immune checkpoint therapies for cancer: implications for precision medicine. *Genome Med*. 2018;10(1):93. doi:10.1186/s13073-018-0605-7
5. Alsaab HO, Sau S, Alzhrani R, et al. PD-1 and PD-L1 checkpoint signaling inhibition for cancer immunotherapy: mechanism, combinations, and clinical outcome. *Front Pharmacol*. 2017;8:561. doi:10.3389/fphar.2017.00561
6. Topalian SL, Drake CG, Pardoll DM. Immune checkpoint blockade: a common denominator approach to cancer therapy. *Cancer Cell*. 2015;27:450–461. doi:10.1016/j.ccell.2015.03.001
7. Pardoll DM. The blockade of immune checkpoints in cancer immunotherapy. *Nat Rev Cancer*. 2012;12(4):252–264. doi:10.1038/nrc3239

8. Sun C, Mezzadra R, Schumacher TN. Regulation and function of the PD-L1 checkpoint. *Immunity*. 2018;48(3):434–452. doi:10.1016/j.immuni.2018.03.014

9. Zou W, Wolchok JD, Chen L. PD-L1 (B7-H1) and PD-1 pathway blockade for cancer therapy: mechanisms, response biomarkers, and combinations. *Sci Transl Med*. 2016;8(328):328rv4. doi:10.1126/sci-translmed.aad7118

10. Xia L, Liu Y, Wang Y. PD-1/PD-L1 blockade therapy in advanced non-small-cell lung cancer: current status and future directions. *Oncologist*. 2019;24(S1):S31–S41. doi:10.1634/theoncologist.2019-IO-S1-s05

11. Borghaei H, Paz-Ares L, Horn L, et al. Nivolumab versus docetaxel in advanced nonsquamous non-small-cell lung cancer. *N Engl J Med*. 2015;373:1627–1639. doi:10.1056/NEJMoa1507643

12. Garon EB, Rizvi NA, Hui R, et al. Pembrolizumab for the treatment of non-small-cell lung cancer. *N Engl J Med*. 2015;372:2018–2028. doi:10.1056/NEJMoa1501824

13. Wang Q, Xu R. Immunotherapy-related adverse events (irAEs): extraction from FDA drug labels and comparative analysis. *JAMIA Open*. 2019;2(1):173–178. doi:10.1093/jamiaopen/ooy045

14. Varricchi G, Galdiero MR, Marone G, et al. Cardiotoxicity of immune checkpoint inhibitors. *ESMO Open*. 2017;2(4):e000247. doi:10.1136/esmoopen-2017-000247

15. Tajiri K, Ieda M. Cardiac complications in immune checkpoint inhibition therapy. *Front Cardiovasc Med*. 2019;6:3. doi:10.3389/fcvm.2019.00003

16. Liu RZ, Fan CX, Zhang ZL, et al. Effects of Dl-3-n-butylphthalide on cerebral ischemia infarction in rat model by mass spectrometry imaging. *Int J Mol Sci*. 2017;18:2451.

17. Tian X, He W, Yang R, Liu Y. Dl-3-n-butylphthalide protects the heart against ischemic injury and H9c2 cardiomyoblasts against oxidative stress: involvement of mitochondrial function and biogenesis. *J Biomed Sci*. 2017;24(1):38. doi:10.1186/s12929-017-0345-9

18. Li J, Li Y, Ogle M, et al. DL-3-n-butylphthalide prevents neuronal cell death after focal cerebral ischemia in mice via the JNK pathway. *Brain Res*. 2010;1359:216–226. doi:10.1016/j.brainres.2010.08.061

19. Abdoulaye IA, Guo YJ. A review of recent advances in neuroprotective potential of 3-N-butylphthalide and its derivatives. *Biomed Res Int*. 2016;2016:5012341. doi:10.1155/2016/5012341

20. Amatore C, Jutand A. Anionic Pd(0) and Pd(II) intermediates in palladium-catalyzed heck and cross-coupling reactions. *Acc Chem Res*. 2000;33(5):314–321. doi:10.1021/ar980063a

21. Wang HM, Zhang T, Huang JK, Sun XJ. 3-N-butylphthalide (NBP) attenuates the amyloid-beta-induced inflammatory responses in cultured astrocytes via the nuclear factor-kappaB signaling pathway. *Cell Physiol Biochem*. 2013;32:235–242. doi:10.1159/000350139

22. Hu Y, Bi X, Zhao P, Zheng H, Huang X. Cytotoxic activities, SAR and anti-invasion effects of butylphthalide derivatives on human hepatocellular carcinoma SMMC7721 cells. *Molecules*. 2015;20 (11):20312–20319. doi:10.3390/molecules201119699

23. Yang M, Dang R, Xu P, et al. Dl-3-n-butylphthalide improves lipopolysaccharide-induced depressive-like behavior in rats: involvement of Nrf2 and NF-kappaB pathways. *Psychopharmacology*. 2018;235:2573–2585. doi:10.1007/s00213-018-4949-x

24. Zhao J, Liu J, Xu E, Liu Y, Xie A, Xiong H. dl-3-n-butylphthalide attenuation of methamphetamine-induced neurotoxicity in SH-SY5Y neuroblastoma cells. *Life Sci*. 2016;165:16–20. doi:10.1016/j.lfs.2016.09.009

25. Liao D, Xiang D, Dang R, et al. Neuroprotective effects of dl-3-n-butylphthalide against doxorubicin-induced neuroinflammation, oxidative stress, endoplasmic reticulum stress, and behavioral changes. *Oxid Med Cell Longev*. 2018;2018:9125601. doi:10.1155/2018/9125601

26. Verdura S, Cuyas E, Cortada E, et al. Resveratrol targets PD-L1 glycosylation and dimerization to enhance antitumor T-cell immunity. *Aging*. 2020;12:8–34. doi:10.18632/aging.102646

27. Kang DY, Sp N, Jo ES, et al. The inhibitory mechanisms of tumor PD-L1 expression by natural bioactive gallic acid in Non-Small-Cell Lung Cancer (NSCLC) cells. *Cancers*. 2020;12:727.

28. Wang Z, Li MY, Zhang ZH, et al. Panaxadiol inhibits programmed cell death-ligand 1 expression and tumour proliferation via hypoxia-inducible factor (HIF)-1alpha and STAT3 in human colon cancer cells. *Pharmacol Res*. 2020;155:104727. doi:10.1016/j.phrs.2020.104727

29. Jie M, Wu Y, Gao M, et al. CircMRPS35 suppresses gastric cancer progression via recruiting KAT7 to govern histone modification. *Mol Cancer*. 2020;19(1):56. doi:10.1186/s12943-020-01160-2

30. MacPherson L, Anokye J, Yeung MM, et al. HBO1 is required for the maintenance of leukaemia stem cells. *Nature*. 2020;577:266–270. doi:10.1038/s41586-019-1835-6

31. Quintela M, Sieglaff DH, Gazze AS, et al. HBO1 directs histone H4 specific acetylation, potentiating mechano-transduction pathways and membrane elasticity in ovarian cancer cells. *Nanomedicine*. 2019;17:254–265. doi:10.1016/j.nano.2019.01.017